Numerical ABL Wind Tunnel Simulations with Direct Modeling of Roughness Elements through Immersed Boundary Condition Method

Bruno Lopez, Gabriel Usera, Gabriel Narancio, Mariana Mendina, Maritn Draper, Jose Cataldo

Abstract Reproduction of atmospheric boundary layer wind tunnel experiments by numerical simulation is achieved in this work by directly modeling, with immersed boundary method, the geometrical elements placed in the wind tunnel's floor to induce the desired characteristics to the boundary layer. The numerical model is implemented on the basis of the open source flow solver caffa3d.MBRi, which uses a finite volume method over block structured grids, coupled with various LES approaches for turbulence modeling and parallelization through domain decomposition with MPI. The Immersed boundary method approach followed the work of Liao et al 2009. Numerical simulation results are compared to wind tunnel measurements for the mean velocity profiles, rms profiles and spectrums, providing good overall agreement. We conclude that the Immersed Boundary Condition method is a promising approach to numerically reproduce ABL Boundary Layer development methods used in physical modeling.

Bruno Lopez,
IMFIA, J. Herrera y Reissig 565, Montevideo, e-mail: brunolop@fing.edu.uy

Gabriel Usera,
IMFIA, J. Herrera y Reissig 565, Montevideo, e-mail: gusera@fing.edu.uy

Gabriel Narancio,
IMFIA, J. Herrera y Reissig 565, Montevideo, e-mail: gnaranci@fing.edu.uy

Mariana Mendina,
IMFIA, J. Herrera y Reissig 565, Montevideo,e-mail: mmendina@fing.edu.uy

Maritn Draper,
IMFIA, J. Herrera y Reissig 565, Montevideo, e-mail: mdraper@fing.edu.uy

Jose Cataldo,
IMFIA, J. Herrera y Reissig 565, Montevideo, e-mail: jcataldo@fing.edu.uy

1 Introduction

The global trend towards urbanisation explains the growing interest in recent decades in studying the Atmospheric Boundary Layer (ABL), comprising the first layer of the atmosphere that extends about 1-2 km from ground and hosts a large part of human activities. The effect of winds on buildings and other structures, as well as on pedestrian in urban environments, the transport of pollutants in air, or wind power generation are a few examples of human activities that develop within the ABL and require its study [3, 9, 2]. The characteristics of the ABL flow are shaped up mainly by the interaction with the ground and so will vary depending on the characteristics of the terrain and its roughness which might correspond for example to different urban environments, sea or vegetated fields [1].

Physically modeling ABL processes in a Wind Tunnel its traditional well stablished technique. Special Wind Tunnels are built for this purpose, named Atmospheric Boundary Layer Wind Tunnels, in which the test sections is preceded by a relatively long working zone in which the modeled ABL flow is developed over selected roughness elements.

While this technique is traditionally used for the study of the ABL, numerical modeling has emerged as a complementary contribution to it in the last decades.The development of modern parallel computers and computational fluid dynamics numerical methods presently allows to numerically simulate turbulent flows with different approaches, ranging from Reynolds Averaged Navier-Stokes methods (RANS), through Large Eddy Simulation (LES), up to Direct Numerical Simulation (DNS) [12].

The Numerical Wind Tunnel methodology targets the numerical simulation of flows which are physically modeled in Wind Tunnels. In the case of the ABL a primary concern in this methodology is to appropriately reproduce the boundary layer characteristics, which in turn are mainly driven by the roughness characteristics of the terrain. Different approaches have been proposed for this matter, including roughness wall functions and drag based representation of vegetation.

This paper aims at a preliminar analysis of viability of using immered boundary method to explicitly representate roughness elements in numerical simulations of ABL Wind Tunnel experiments. Chapter 2 presents the reference Wind Tunnel experiments used for comparision with the numerical simulations developed in this work. Chapter 3 presents the numerical method, describing the base open source solver used, caffa3d.MBRi, as well as the immersed boundary approach followed to represent roughness elements. Chapter 4 presents the results and conclusions are derived in Chapter 5.

2 Wind tunnel experiments

The experimental data used in this work was obtained at the Atmospheric Boundary Layer Wind Tunnel of the Facultad de Ingenieria in Uruguay, which is an open

circuit wind tunnel with a 2.20×2.25 m square test section, and a 14 m long inlet region for the development of the ABL, capable of achieving maximum wind speeds of 30 m/s. In figure 1 the general layout of the Wind Tunnel is presented.

Boundary layer development is shaped up with a series of cubical elements, 3 cm in side, placed in a regular staggered arrangement with a 15 cm spacement, 3 Standen spires type vortex generators [14], of 134 cm height, and a 31.5 cm height wall placed at the inlet. This arrangement is used to reproduce an urban boundary layer with a length scale 1:200. Figure 2 gives general and detailed views of this arrangement.

Velocity was measured with a TSI IFA 100 hot wire anemometer. SN hot film probes were used for this purpose. The sampling rate was 4000 Hz and a low-pass filtering of the signal at 2000 Hz was used to avoid aliasing. 65536 samples were taken in each location accounting to a sampling time of 16,384 s. The positioning of the hot film probe was done using a robotic arm designed to perform this task. Vertical profiles of mean velocity, root mean square fluctuations are obtained as well as power spectrums at selected locations. Experimental results are reported and compared with numerical simulation results in section 4.

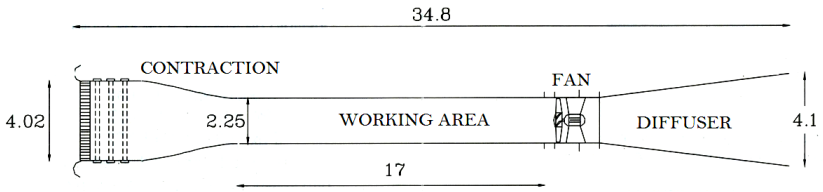

Fig. 1 Layout of the Atmspheric Boundary Layer Wind Tunnel at IMFIA. Lengths in (m)

Fig. 2 General (left) and detalied (right) views of the wind tunnel test section and boundary layer preparation section, with roughness element cubes and vortex induction Standen spires type elements

3 Numerical method

The methodology developed to numerically simulate atmospheric boundary layer wind tunnel tests is based on the open source solver caffa3d.MBRi [10], coupled with a specific immersed boundary conditions module, following the work of [7], to explicitly represent the geometry of roughness elements used in the Wind Tunnel.

The open source incompressible flow solver caffa3d.MBRi is a Fortran90 implementation of the finite volume method, evolved from the work of Ferziger and Peric [4]. It features a block structured framework to accommodate both a flexible approach to geometry representation and a straightforward implementation of parallel capabilities through the MPI library. Representation of complex geometries can be handled semi automatically through a combination of body fitted blocks of grids and the immersed boundary condition strategy over both Cartesian and body fitted grid blocks. The parallelization strategy is based on the same block structured framework, by means of encapsulated MPI calls performing a set of conceptually defined high level communication tasks. It has been suggested by other authors that fluid dynamics research would benefit from the availability of more public and open source codes [17]. The authors agree with this view and welcome the use and further development of caffa3d.MBRi model by other researchers. For this purpose the code is freely available through the website (www.fing.edu.uy/imfia/caffa3d.MB).

3.1 Mathematical model

The mathematical model comprises the mass balance equation (1) and momentum balance equation (2) for a viscous incompressible fluid, together with generic non-reacting scalar transport equation (3) for scalar field ϕ with diffusion coefficient Γ. Note that (2) has been written only for the first Cartesian direction here.

$$\int_S (v \cdot \hat{n}_S)\, dS = 0 \tag{1}$$

$$\int_\Omega \rho \frac{\partial u}{\partial t} d\Omega + \int_S \rho u\, (v \cdot \hat{n}_S)\, dS = \int_\Omega \rho \beta \left(T - T_{ref}\right) g \cdot \hat{e}_1 d\Omega + \int_S -p \hat{n}_S \cdot \hat{e}_1 dS + \int_S (2\mu D \cdot \hat{n}_S) \cdot \hat{e}_1 dS \tag{2}$$

$$\int_\Omega \rho \frac{\partial \phi}{\partial t} d\Omega + \int_S \rho \phi\, (v \cdot \hat{n}_S)\, dS =$$

$$\int_S \Gamma \left(\nabla \phi \cdot \hat{n}_S\right) dS \tag{3}$$

In these equations, $v = (u, v, w)$ is the fluid velocity, ρ is the density, β is the thermal expansion factor, T the fluid temperature and T_{ref} a reference temperature, g is the gravity, p the pressure, μ the dynamic viscosity of the fluid and D the strain tensor. The balance equations are written for a region Ω, limited by a closed surface S, with unit outward pointing normal $\hat{n}_S$. Finally $\hat{e}_1$ is the first Cartesian direction.

The generic transport equation (3) for non-reacting scalars can be used to implement in a straightforward manner further physical models like heat transport required for the temperature field, both Reynolds Averaged and Large Eddy Simulation turbulence closures, wet air processes which include evaporation and condensation, etc. An arbitrary number of scalar fields can be solved simultaneously, with coupling between them as for the case of temperature field influencing both momentum equations through buoyancy and wet air process equations through condensation and evaporation conditions. The use of equations in their global balance form together with the finite volume method, as opposed to the differential form, favors enforcing conservation laws for fundamental quantities such as mass and momentum into the solving procedure [4]. For the present simulations a standard Smagorinsky large eddy turbulence model was attached to the solver.

3.2 Discretization and solving procedure

Complete details for discretization of each term will not be given here but can be found in [16], together with various validations of the solver [16, 15, 10]. Second order central differencing scheme for diffusive terms is used, while convective terms are discretized blending first order upwind approximations and second order central differences.

Further, the SIMPLE [13] method for pressure-velocity coupling is used to obtain a discretized equation for the pressure, from the mass balance equation (1). Refined methods for pressure-velocity coupling can also be incorporated [6], together with improved linear interpolations [5]. Also different implicit time stepping schemes can be combined for the momentum equations, like first order backwards Euler or second order Cranck-Nicholson.

The usual lexicographical order in 3D implies that the resulting segregated linear equation system is hepta-diagonal in each grid block, and thus globally block hepta-diagonal. Either a block structured variant of the Stone-SIP solver [8] or a block structured Algebraic Multigrid (AMG) solver with SIP as a smoother [11, 16] are used for iterative solution of each linear system. The SIP solver algorithm accommodates well the block structure inherited from the grid, allowing efficient parallelization.

3.3 Immersed boundary conditions method

Following the work of [7], a specific immersed boundary conditions module was included in the solver. In this approach the geometry of roughness elements used in the Wind Tunnel, like cubes and spires, is explicitly represented over the structured grid, by means of a triangulated surface as shown in figure 3, The distance from each grid node to the closest roughness element wall is then computed and used to derive the forcing term. For grid nodes that fall inside roughness elements an additional body force term is computed to enforce null velocity at that node. For grid nodes falling outside roughness elements, but close enough, an interpolation procedure is applied to estimate the target velocity at the node and the additional body force is applied based on that estimate. This computation is embeded into the overal implicit outer iteration procedure, so that the additional body force value at each node is adjusted within each time step until convergence is reached.

This procedure leads to an almost automatic meshing strategy for a geometry in which developing a body fitted block structured grid would be seldom feasible. Unstructured grids would be better suited for a body fitted approach, but still would require considerable meshing effort, especially considering the intricate global geometry of the roughness elements set. Also, modifying the geometry of roughness elements can be done on the fly, without requiring a change in the grid.

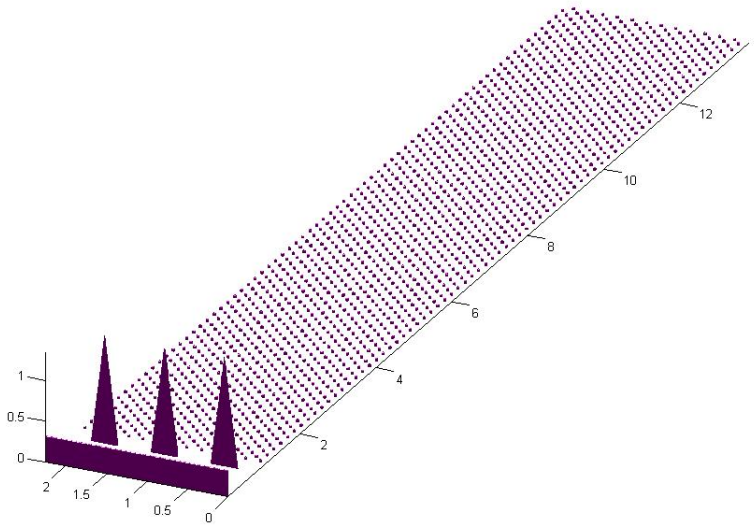

Fig. 3 Immersed Boundary Condition representation of roughness element cubes and vortex induction Standen spires type elements.

While the grid resolution does not warrants that the boundary layer over each individual roughness element will be adequately captured, it is expected that the overall contribution to the development of the ABL like flow, comprised of the superposition of each elements wakes, will be indeed well represented.

3.4 Numerical simulations setup

The computational domain corresponds to the working area of the wind tunnel, 13.72 m long up to the test section, within which the boundary layer is developed. Buffer regions for inlet and outlet boundary conditions add up to the total length of 16.25 m for the computational domain, with a cross section 2.25 m wide and 2 m high. This domain was split into 26 identical regions or grid blocks, each 1.25 m long, 1.125 m wide and 2m high. Two grids were setup with different spatial resolution. For the coarse grid, a uniform horizontal grid spacing of 1.56 cm was used. A vertical non-uniform distribution of cells was selected, with minimum vertical spacing of 1mm at the floor. Each grid block then required 80 cells in the streamwise direction, 72 cells spanwise and 104 cells in the vertical, for a total of almost 600.000 cells per grid block. For the fine grid, the horizontal resolution was set to 1.04 cm while the vertical resolution was kept at 1mm at the floor. The total number of cells per grid block for the fine grid was about 2 million cells, 120 cells streamwise, 108 cells spanwise and 156 in the vertical direction.

Wall boundary conditions with non slip condition were applied at the floor, while slip conditions were applied at the roof and side walls of the tunnel. The inlet was set to a uniform velocity of Uo=13.5 m/s and null gradient boundary condition normal to the outlet was applied.

For the coarse grid a time step of 0.5 seconds was used, while for the fine grid computations were performed for time steps of 0.5 s and 0.01 s. Computations were distributed in 26 cores on the Cluster-FING infraestructure [www.fing.edu.uy/cluster]. A total of about 60.000 cpu-hours were used for the set of numerical simulations with an estimated cost of about less than one thousand euros.

4 Results

Mean velocity profiles from Wind Tunnel experimental data and from the three numerical simulation runs are presented in figure 4, showing good agreement between numerical and experimental data, as well as almost grid and time step independance. Preliminary analysis, not indluded here due to sapce constrains, also show a good logarithmic behaviour at the logarthmic sublayer. In figure 5, urms profiles are given for the same set of experimental and numerical data, showing a good match as well.

Finally, power spectrums for longitudinal velocity are given at 100mm from floor for experimental data in figure 6 and for numerical results from the fine grid in figure

7. The behaviour of numerical results up to the integral scales and the begining of the inertial sub-ranges is appropriate, while the energy decay afterwards is more accentuated, probably due to too much dissipation from the LES model, with an early sharp cut off due to grid resolution.

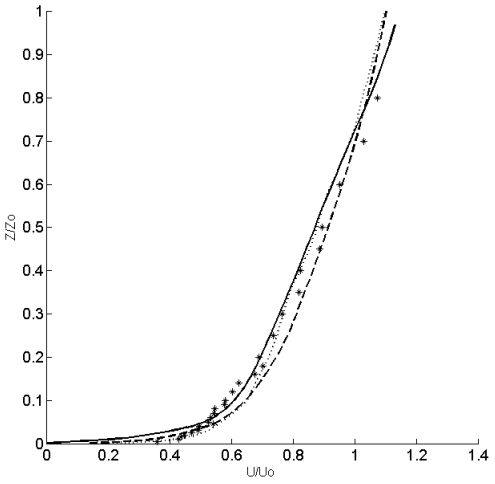

Fig. 4 Mean velocity profiles form experiments and numerical simulations. symbols: experimental data; solid line: coarse grid dt=0.5s; dashed line: fine grid dt=0.5s; dotted line: fine grid dt=0.01s

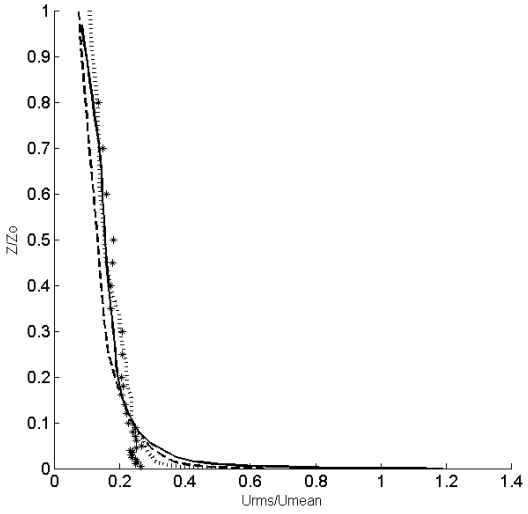

Fig. 5 Urms profiles form experiments and numerical simulations. symbols: experimental data; solid line: coarse grid dt=0.5s; dashed line: fine grid dt=0.5s; dotted line: fine grid dt=0.01s

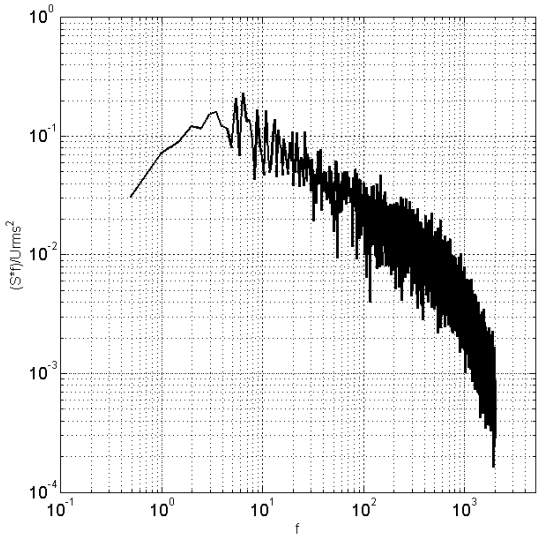

Fig. 6 Power spectrum for longitudinal velocity at 100m height, from experimental data

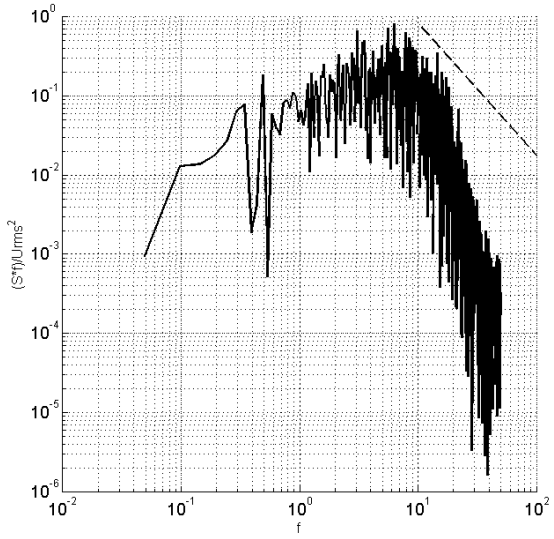

Fig. 7 Power spectrum for longitudinal velocity at 100m height, from fine grid numercial simulations

5 Conclusions

Preliminary results showing good overall agreement between experimental data and numerical simulations suggest that the direct representation of roughness elements by immersed boundary condition method is an effective way of numerically modeling ABL Wind tunnel tests. Both mean velocity profile and urms profile were adequately captured at the applied grid resolutions, which must be fine enough to

geometrically resolve the roughness elements. While computational intensive the proposed method has the advantage of requiring almost no calibration to reproduce wind tunnel test conditions. Almost no meshing effort is required as well, making it possible to even use a single grid for different roughness element setups.

Acknowledgements This work was supported by grant FSE-2011-6015 from ANII

References

1. Bitsuamlak,G.T, Stathooulos, T., Bedard, C. *Numerical evaluation of wind flow over complex terrain: review.* (2004)
2. Blocken, B. and Carmeliet, J., *A review of wind-driven rain research in building science.* Journal of Wind Engineering and Industrial Aerodynamics (2004) 92 (13), 1079-1130
3. Dayan E. Wind energy in buildings: Power generation from wind in the urban environmentwhere it is needed most. Refocus 7(2), 338 (2006)
4. Ferziger J. and Peric M., *Computational methods for fluid dynamics*. (Springer-Verlag), (2002).
5. Lehnhauser T. and Schäfer M., Improved linear interpolation practice for finite-volume schemes on complex grids. *International Journal for Numerical Methods in Fluids*, 38 (2002) 625-645.
6. Lehnhauser T. and Schäfer M., Efficient discretization of pressure-correction equations on non-orthogonal grids. International Journal for Numerical Methods in Fluids, 42 (2003) 211-231.
7. Liao C., Chang Y., Lin C., McDonough J.M., *Simulating flows with moving rigid boundary using immersed-boundary method.* Computers and Fluids, 39 (2010) 152-167.
8. Lilek Z., Muzaferija S., Peric M., Seidl V., An implicit finite-volume method using nonmatching blocks of structured grid. Numerical Heat Transfer, Part B, 32 (1997) 385-401.
9. Meroney, R. N., Wind tunnel numerical simulations of pollution dispersion: a hybrid approach. Working paper, Croucher Advanced Study Institute on Wind tunnel Modelling, Hong Kong University of Science and Technology, 6-10. (2004), 60pp
10. Mendina M., Draper M., Kelm Soares A.P., Narancio G., Usera G. A general purpose parallel block structured open source incompressible flow solver. Cluster Computing 17(2): 231-241 (2014)
11. Mora Acosta J., Numerical algorithms for three dimensional computational fluid dynamic problems. *PhD Thesis, UPC*, (2001).
12. Pope, S. B. Turbulent Flow Cambridge University Press, Cambridge, UK, (2001)
13. Rhie C.M., Chow W.L., A numerical study of the turbulent flow past an isolated airfoil with trailing edge separation. AIAA Journal, 21 (1983) 1525-1532.
14. Standen N.M. A spire array for generating thick turbulent shear layers for natural wind simulation in wind tunnels National Research Council Canada, Aeronautical Establishment report no. LTR-LA-94 (1972)
15. Usera G., Vernet A., Ferré J. A., Use of time resolved PIV for validating LES/DNS of the turbulent flow within a PCB enclosure model. *Flow, Turbulence and Combustion*, 77 (2006) 77-95.
16. Usera G., Vernet A., Ferré J. A., A Parallel Block-Structured Finite Volume Method for Flows in Complex Geometry with Sliding Interfaces. *Flow, Turbulence and Combustion*, 77 (2008) 471-495.
17. Zaleski S., Science and Fluid Dynamics should have more open sources. *http://www.lmm.jussieu.fr/˜zaleski/OpenCFD.html*, (2001)